

# Seismic Response Reduction of a Building Using Top-Story Isolation System with MR Damper

Hyun-Su Kim

Division of Architecture, Sunmoon University, Asan-si, Korea

Copyright © 2014 Hyun-Su Kim. This is an open access article distributed under the Creative Commons Attribution License, which permits unrestricted use, distribution, and reproduction in any medium, provided the original work is properly cited.

## Abstract

In this study, the adaptability of a semi-active top-story isolation system with an MR damper for reduction of seismic responses of tall buildings has been investigated. To this end, a 20-story building structure was selected as an example. Low damping elastomeric bearings and an MR damper were used to compose a smart top-story isolation system. Artificial earthquakes generated based on design spectrum were used for structural analyses. A fuzzy logic controller (FLC) was used to control an MR damper and the FLC was optimized by multi-objective genetic algorithms (MOGA). Numerical simulations show that a smart top-story isolation system can effectively reduce both structural responses and isolation story drifts of the building structure compared to a passive system.

**Keywords:** Vibration control, Semi-active control system, Top-story isolation, Seismic response reduction, Genetic algorithms, Multi-objective optimization

## 1 Introduction

The use of a base isolation system is a well-known approach in the seismic design of low-rise buildings. However, for technical reasons, this base isolation system cannot be effectively applied to high-rise buildings [1, 2]. The natural periods of tall buildings are relatively long, and changing the first mode of vibration requires a large flexibility in the isolation mechanism. This is considered a major technical problem, especially if a large misalignment of vertical force on the isolator is expected. The vertical stiffness of the isolator is also a technical concern. Based on these problems, a top- or mid-story seismic isolation system has been proposed [3, 4, 5]. The isolated upper stories of the tall building structure

with a top- or mid-story seismic isolation system are rolled to act as a large tuned mass damper (TMD). Recently, smart base isolation strategies have been widely studied as novel mitigation techniques to reduce structural damage caused by severe loads. Current literature shows that a smart base isolation system can reduce base drifts without accompanying increases in acceleration that are seen with passive strategies [6, 7]. Several researchers have investigated the use of semi-active smart dampers for seismic response mitigation as a component of a hybrid control system [7, 8]. Control methodologies for these semi-active smart base isolation systems include fuzzy control [8], sliding mode control [9], clipped-optimal control [7], and others. It has been shown that smart base isolation can protect low-rise building structures in extreme earthquakes without sacrificing performance during more frequent, moderate seismic events. However, a smart top-story isolation system for tall buildings has not been fully investigated to date. Therefore, the control performance of a smart top-story isolation system for a building structure subjected to seismic excitation was investigated in this paper. A smart top-story isolation system consists of MR dampers and low damping elastomeric bearings and a fuzzy logic controller (FLC) was used to control an MR damper [10]. A multi-objective genetic algorithm (MOGA) was selected to optimize the fuzzy rules and membership functions of FLC.

## 2 Analytical models and artificial earthquake load

In this study, a typical 20-story building, as shown in Figure 1(a), and an example building with a smart top-story isolation system, as shown in Figure 1(b), are employed as example structures for evaluating the control performance of a smart top-story isolation system. Each building is represented by a shear building model with 20 DOFs. As shown in Figure 1(b), a smart top-story isolation system consists of an MR damper and elastic bearings. In order to compare the control performance of a smart top-story isolation system, a passive top-story isolation system is used. In the passive system, an MR damper, as shown in Figure 1(b) is replaced by a proper viscous damper.

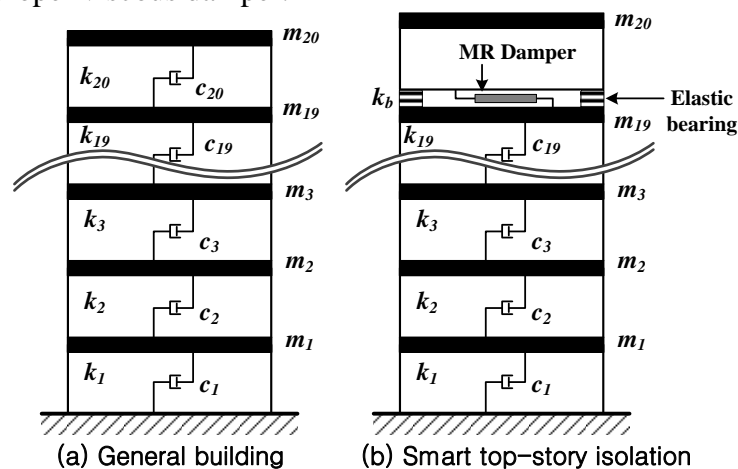


Figure 1. Analytical model of 20-story example structure

The equations of motion of the general building and the top-story isolated building are given by equations (1) and (2).

$$M\ddot{x}_1 + C_1\dot{x}_1 + K_1x_1 = -ME\ddot{x}_g \quad (1)$$

$$M\ddot{x}_2 + C_2\dot{x}_2 + K_2x_2 = -ME\ddot{x}_g + E^F F_C \quad (2)$$

where  $E$  is a unit vector with a size of  $[20 \times 1]$  for applying ground acceleration to each story mass,  $F_C$  is the MR damper force in the smart top-story isolation system and  $E^F$  is a location vector of the isolation system. This location vector contains '1' element for the top story and '0' elements for the other stories. In the equations,  $x_1, \dot{x}_1, \ddot{x}_1$  and  $x_2, \dot{x}_2, \ddot{x}_2$  are the displacement, velocity and acceleration of the general building and the top-story isolated building, respectively, and  $\ddot{x}_g$  represents the ground acceleration.  $M$  is the 20 by 20 dimensional mass matrix for both the general building and top-story isolated building. It is represented by a typical diagonal matrix with the diagonal element,  $m_i$ , that is the mass of the  $i$ th floor ( $i=1,2,\dots,20$ ) and is  $8 \times 10^5$  kg.

$K_1$  and  $K_2$  are the stiffness matrices of the general building and the top-story isolated building, respectively. In this example, the stiffness coefficient of each floor ( $k_i$ ) is  $1.35 \times 10^9$  N/m. In general, a top-story isolation system provides the best control performance when its dynamic behavior is similar to a tuned mass damper (TMD). Generally, the frequency of a TMD is tuned to the first modal frequency of the structure because the motion of a long period structure is generally governed by the first modal response. Accordingly, the stiffness coefficient ( $k_b$ ) of the elastic bearing shown in Figure 1(b) is selected to tune the frequency of the isolated top-story structure to the first modal frequency of the substructure (i.e., 19-story building structure without a top story). The first five natural periods of the 20-story building are 2.00, 0.67, 0.40, 0.29 and 0.23 sec.  $C_1$  and  $C_2$  are the damping matrices of the general building and the top-story isolated building, respectively, and are defined using Rayleigh damping. Classical Rayleigh damping is assumed for the example building with a 2% critical damping ratio in the first two modes. Optimal parameters for the design of a passive TMD proposed by Warburton [11] are employed as shown in equation 3 for passive top-story isolation system. In this equation, the parameter  $\mu$  refers to the mass ratio of TMD with respect to the main structure, and is 5.26%. The optimal damping ratio for the passive top-story isolation system is calculated to be 11.25% using equation (3).

$$\sqrt{\frac{\mu(1 - \mu/4)}{4(1 + \mu)(1 - \mu/2)}} \quad (3)$$

As shown in Figure 2, the Bouc-Wen model [12] was used to describe how the

damping force is related to the velocity and applied command voltage. The MR damper model has a maximum generated force of about 500 kN, depending on the relative velocity across the MR damper with a saturation voltage of 5 V.

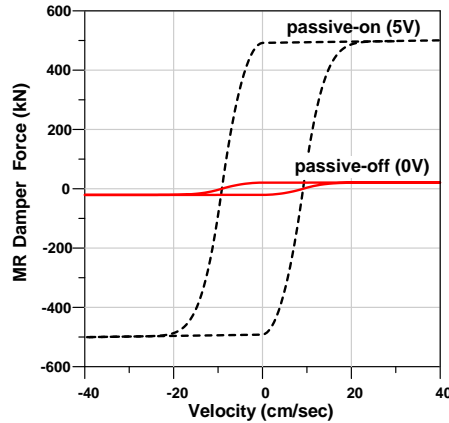


Figure 2. Force-velocity relationship of MR damper

In numerical analysis, the model of the example structure is subjected to an artificial ground motion. An artificial earthquake record was created to fit the design response spectrum, representing the seismic characteristics in the regions of low-to-moderate seismicity using the SIMQKE software program [13]. Figure 3 shows the acceleration time history graph of the artificial earthquake. The peak ground acceleration (PGA) of the artificially-generated earthquake was 0.144g, which suggests that the artificial earthquake represents the ground motions for regions of low-to-moderate seismic activity. The artificial ground motion was generated with a time step of 0.01 seconds and its duration was 30 seconds.

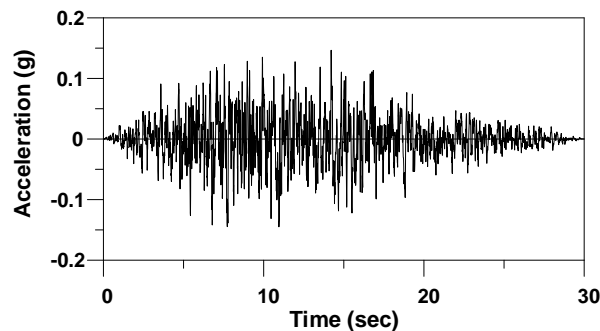


Figure 3. Acceleration time history of an artificial earthquake

### 3 Development of control algorithm for smart top-story isolation

As explained previously, the FLC is used to control the smart top-story isolation system. In the FLC, the 19th floor acceleration and the isolator drift are selected for two input variables and the output variables are the command voltages sent to the MR damper. Fuzzy rules and membership functions are opti-

mized using a multi-objective genetic algorithm (MOGA). The reduction of the peak drift of the isolator and the RMS acceleration of the 19th floor are selected as two objectives in a multi-objective optimization process. Each response controlled by the MOGA-optimized FLC is normalized by the corresponding response of the building with a passive top-story isolation system in each objective function. Therefore, if the calculated objective function values are less than 1, the control performance of the smart top-story isolation system is better than that of the passive top-story isolation system. The optimization process of MOGA is presented in Figure 4.

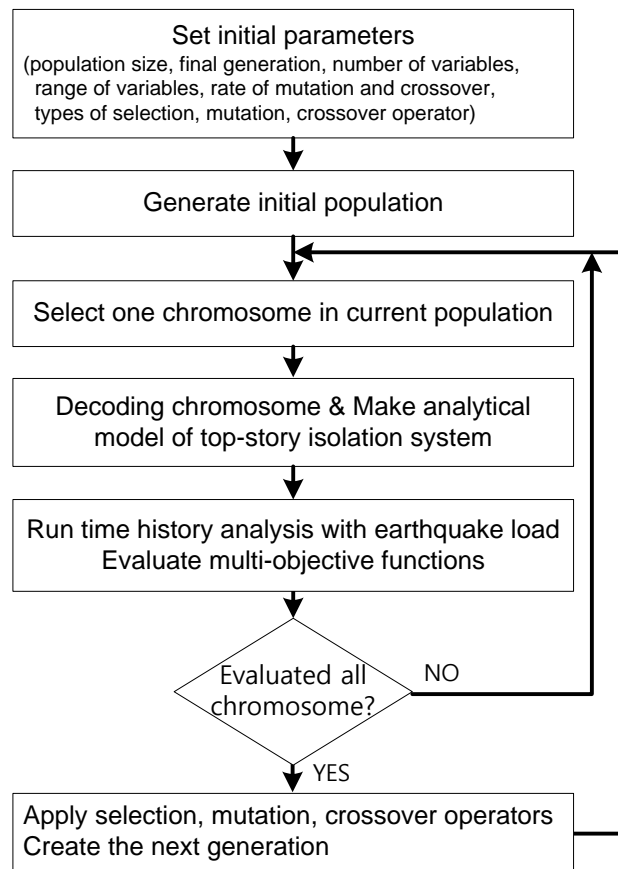


Figure 4. MOGA optimization process

#### 4 Control performance evaluation of top-story isolation system

A numerical model of the 20-story example building structure with a smart top-story isolation system is implemented in SIMULINK and MATLAB. The MOGA based optimization is performed with the population size of 100 individuals. The upper limit on the number of generations is specified to be 1000. As the number of generations increases, the control performance of the elite (i.e. non-dominated) individuals is improved. After the optimization run, the Pareto-optimal front (a set of Pareto-optimal solutions) is obtained as shown in

Figure 5. Figure 5 shows that the  $J_1$  and  $J_2$  of each solution are less than 1; the smart top-story isolation system can therefore provide better control performance in reducing both the isolation story drift and the 19<sup>th</sup> story acceleration compared to the passive system. Consequently, one controller, that can appropriately control both the isolator drift and the 19<sup>th</sup> floor acceleration responses, has been selected among the Pareto optimal FLCs.

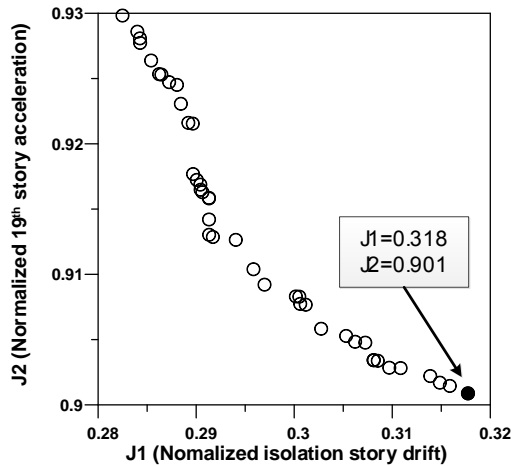


Figure 5. Pareto optimal solutions

The values of  $J_1$  and  $J_2$  of the selected FLC (marked as a solid circle in Figure 5) are 0.318 and 0.901, respectively. Accordingly, the smart top-story isolation system controlled by the selected FLC can reduce the peak drift of the isolator and RMS 19<sup>th</sup> story acceleration by approximately 68% and 10%, respectively, compared to the passive top-story isolation system. The peak displacement of the 20<sup>th</sup> story with a passive isolation system is 22.1 cm as shown in Figure 6. This can be reduced by more than 50% (i.e. 10.9 cm) when a smart isolation system is used. Because the RMS accelerations of the isolated story with the smart system are also less than those of the passive system, it is expected that the smart control system increases the safety of the building structure with a top-story isolation system. The smart top-story isolation system can effectively reduce both the peak displacements and the RMS accelerations of the main structure below the isolation story as shown in Figure 7.

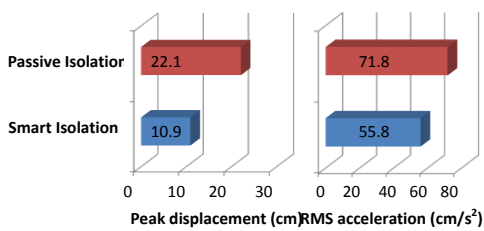


Figure 6. 20<sup>th</sup> story responses

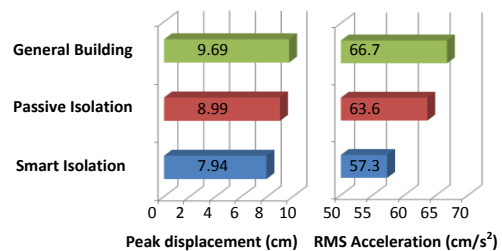


Figure 7. 19<sup>th</sup> story responses

The isolator drift and the 19<sup>th</sup> story acceleration time histories of the passive and smart isolation systems are presented in Figures 8 and 9, respectively. The isolation story drift, which is closely related to the safety of a top-story isolation system, can be considerably reduced by the smart isolation system. If additional damping devices are used in the passive isolation system, the isolation story drift can be reduced. However, the addition of damping may deteriorate control performance of the top-story isolation system. Consequently, a smart top-story isolation system can effectively reduce the seismic responses of both the main structure and the isolated top story.

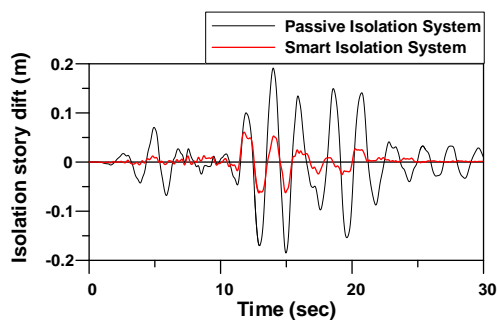


Figure 8. Isolator drift

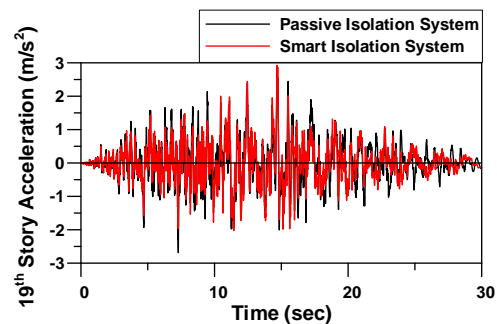


Figure 9. 19th story acceleration

## 5 Conclusions

In this study, a smart top-story isolation system consisting of an MR damper and low damping elastomeric bearings was proposed to reduce the seismic responses of a building structure. A fuzzy logic control algorithm was developed to effectively control the smart top-story isolation system using a multi-objective genetic algorithm. Both the isolator drift and acceleration response of the example structure were used as objective functions for the multi-objective optimization problem. The optimally-designed passive system was used as a reference for a comparative study. Based on numerical simulations, it can be seen that the smart top-story isolation system can effectively reduce both the main structure and the isolated top story responses compared to the passive top-story isolation system. The MOGA-optimized FLC shows good performance for controlling smart top-story isolation. After a single optimization run using MOGA, an engineer can simply select another FLC that satisfies the desired performance requirements from among a number of Pareto optimal solutions. This may be the most important characteristic of the MOGA based optimization compared to other optimization methods. It is expected that a top-story isolation system is an effective means for mitigating the seismic-induced responses of a tall building.

**Acknowledgements.** This work was supported by a National Research Foundation of Korea (NRF) grant funded by the Korea government (MEST) (NRF-2013R1A1A2058312).

## References

- [1] F. Naeim and J.M. Kelly, *Design of Seismic Isolated Structures: from Theory to Practice*. Wiley: New York. (1999).
- [2] J.M. Kelly, The current state of base isolation in The United States, *Proc. 2nd World Conference on Structural Control*, Kyoto, Japan, (1999), 1043-1052.
- [3] M. Ziyaeifar and H. Noguchi, Partial mass isolation in tall buildings, *Earthquake Engineering and Structural Dynamics*, **27** (1998), 49-65.
- [4] X. Huang, F. Zhou, S. Wang and X. Luo, Theoretical and experimental investigation on mid-story seismic isolation structures, *The 14th World Conference on Earthquake Engineering*, Beijing, China, (2008).
- [5] R. Villaverde, Implementation study of aseismic roof isolation system in 13-story building, *Journal of Seismology and Earthquake Engineering*, **2** (2000), 17-27.
- [6] B.F. Spencer, Jr. and S. Nagarajaiah, State of the art of structural control, *Journal of Structural Engineering*, ASCE, **129** (2003), 845-856.
- [7] B.F. Spencer, Jr., E.A. Johnson and J.C. Ramallo, Smart isolation for seismic control, *JSME International Journal Series C*, **43**, (2000), 704-711.
- [8] H.S. Kim and P.N. Roschke, GA-fuzzy control of smart base isolated benchmark building using supervisory control technique, *Advances in Engineering Software*, **38** (2007), 453-465.
- [9] J. N. Yang, J. C. Wu, A. M. Reinhorn and M. Riley, Control of sliding-isolated buildings using sliding-mode control, *Journal of Structural Engineering*, **122** (1996), 179-186.
- [10] L.M. Jansen and S.J. Dyke, Semi-active control strategies for MR dampers: a comparative study", *Journal of Engineering Mechanics*, ASCE, **126** (2000), 795-803.
- [11] G.B. Warburton, Optimum absorber parameters for various combinations of response and excitation parameters, *Earthquake Engineering and Structural Dynamics*, **10** (1982), 381-401.
- [12] R.H. Sues, S.T. Mau and Y.K. Wen, System Identification of Degrading Hysteretic Restoring Forces, *Journal of Engineering Mechanics*, ASCE, **114**, (1988), 833- 846.
- [13] E.H. Vanmarcke and D.A. Gasparini, *SIMQKE: A program for artificial motion generation*, Dept. of Civil Engineering, Massachusetts Institute of Technology, (1976).

**Received: September 1, 2014**